

# Diversity of dynamic voltage patterns in neuronal dendrites revealed by nanopipette electrophysiology

Jeffrey Mc Hugh<sup>1,2,\*</sup>, Stanislaw Makarchuk<sup>3,\*</sup>, Daria Mozheiko<sup>1,4</sup>, Ana Fernandez-Villegas<sup>3</sup>,  
Gabriele S. Kaminski Schierle<sup>3</sup>, Clemens F. Kaminski<sup>3</sup>, Ulrich F. Keyser<sup>2</sup>, David Holcman<sup>5,6,†</sup>,  
Nathalie Rouach<sup>1,6,†,††</sup>

<sup>1</sup>Center for Interdisciplinary Research in Biology, Collège de France, CNRS, INSERM,  
Université PSL, Labex Memolife, Paris, France

<sup>2</sup>Cavendish Laboratory, University of Cambridge, Cambridge CB3 0HE, United Kingdom

<sup>3</sup>Department of Chemical Engineering and Biotechnology, University of Cambridge, Philippa  
Fawcett Drive, Cambridge CB3 0AS, United Kingdom

<sup>4</sup>Doctoral School N°158, Sorbonne Université, Paris, France

<sup>5</sup>Group Data Modelling, Computational Biology and predictive medicine, Institut de Biologie  
de l'Ecole Normale Supérieure, CNRS, INSERM, Université PSL, Labex Memolife, Paris,  
France

<sup>6</sup>Churchill College, Cambridge CB3 0DS, United Kingdom

\* These authors contributed equally

† These authors contributed equally

††To whom correspondence should be addressed: [nathalie.rouach@college-de-france.fr](mailto:nathalie.rouach@college-de-france.fr)

## Supporting Information

### **1. Nanopipette conductance model:**

Below is the derivation underlying equation 1 the main text, which we used in conjunction  
with resistance measurements to estimate the aperture of each nanopipette.

The geometry of a glass nanopipette is shown in Fig. S1. We treat the pore as a conical  
frustum, with a diameter  $d$  at the tip and  $D$  at the base. The conical pore has a length  $L$  (taper  
length), with an angle  $\alpha$  so that:

$$\tan \alpha = \frac{D - d}{2L} \quad (\text{SE1})$$

Ohm's law states that

$$J = \sigma E = \frac{I}{\pi r(x)^2}, \quad (\text{SE2})$$

for a current density  $J$  (current per cross-sectional area), conductivity  $\sigma$  and an electric field  $E$ .  
The radius of the cone at an axial position  $x$  is given by the relation:  $r(x) = 0.5d + x \tan(\alpha)$ . The

conductance  $G$  of the nanopipette can be calculated by integrating the electric field when a current  $I$  is injected by integrating the field

$$G = \frac{I}{V} = I \left( \int_0^L E dx \right)^{-1} = \left( \int_0^L \frac{1}{\pi \sigma (d/2 + x \tan(\alpha))^2} dx \right)^{-1} \quad (\text{SE3})$$

$$= \left( \frac{4L}{2L \tan(\alpha) + d^2} \right)^{-1} \left( \frac{1}{\pi \sigma} \right)^{-1} = \frac{\pi \sigma (2L \tan(\alpha) + d^2)}{4L} = \frac{\pi \sigma d D}{4L}.$$

We used that  $2L \tan(\alpha) = D - d$ . Taking access resistance into account [REF], we refine this expression to become:

$$G = \frac{\pi \sigma d D}{4(L + 0.8(d + D))} \quad (\text{SE4})$$

Rearranging in terms of  $d$  gives:

$$d = \frac{(3.2DG + 4LG)}{(\pi \sigma D - 3.2G)}. \quad (\text{SE5})$$

This result is equation 1.

## 2. Data Analysis

### Segmentation of single spontaneous event detection

Events were detected and isolated as follows: all peaks were detected using the standard *findpeaks* function with baseline below -50 mV. Then, peaks with amplitude below 10 mV were filtered out. To remove local maxima, we searched for peaks which are spaced from each other with  $\Delta t < 5$  ms. Finally, a list of timestamps associated to the peaks was collected. To find the initial time for these events, we identified the sharp rise of the membrane voltage. By computing the first derivative of the signal before the peak within a time window of 2 ms. The corner was defined at the point where the value of the derivative exceeded a threshold value of 10 mV/ms. Event termination was defined in a similar way, but with a 5 ms time window, and the signal was cropped at the first point where the absolute value of the derivative of the signal became less than 0.1 mV/ms. The values for the time windows and thresholds were chosen empirically based on visual inspection of the output results, using a custom written MatLab routine. The rise time was defined as the time between the beginning of an event and its peak. Similarly, the signal amplitude was defined as the difference between the value of the peak and the minimum value of the first time point at single event. The baseline was defined as an average value of the signal at the first and the last time point of an event, and the decay trend was fitted with an exponential function;  $f(t) = e^{-t/\tau_{fit}}$ , where the characteristic  $\tau_{fit}$  was fitted to data. In total, 7537 spontaneous events were identified from 3 recordings lasting 2500 s, 3477 s and 4299 s obtained from cultured hippocampal rat neurons and 2882 events were identified from 5 recordings (all between 5 and 15 minutes long) of mice cultured neurons in the pro-bursting solution.

### Burst segmentation

Bursts were manually isolated from 5 traces recorded from mice neurons. The number of events in a burst was defined using the MatLab function *findpeaks*, and like the single event analysis, the peaks with a prominence less than 10 mV were filtered out. The burst amplitude was computed as the difference between the voltage of the highest peak and the baseline, which was extracted as an average value of the signal at the first and the last time point of an event. The duration  $\Delta T_{burst}$  was computed as the time difference between neighboring single peaks in one burst. In total, 445 bursts were analyzed.

#### **Interburst interval and silent phase**

Silent time periods were defined as the sections of traces where:

- (i) No peaks with a prominence above 5 mV were detected and
- (ii) The first derivative of the signal at any point within a window of 10 ms did not exceed 5 mV/ms.

The baseline of silent regions was determined as the mean value of voltages within one subtrace. To compute the derivative, a time window of 10 ms was chosen, corresponding to the minimum duration of silent regime subtraces detected. In total 18969 (rat) and 3536 (mice) silent epochs were identified. The mean duration of the silent regime was determined to be  $31 \pm 1$  ms in rats and  $63 \pm 12$  ms in mice and the mean frequency (in events per minute) of the silent regime observed in rats was  $96.5 \pm 51.1$  and in mice was  $69.4 \pm 32.9$ .

#### **Active regime segmentation**

We identified transient firing events, defined as subtraces where at least 4 transient events with an amplitude >15 mV were detected during a time window of 100 ms. The baseline of the firing regions was defined as an average of valley values detected between peaks. We selected 195 firing periods from mouse neurons, and 2702 from rat neurons for analysis. We measured the mean duration of the active regime to be  $121 \pm 3$  ms in rats and  $529 \pm 78$  ms in mice. The mean frequency of the active regime was calculated to be  $13.8 \pm 6.6$  in rats and  $5.4 \pm 1.2$  in mice.

#### **Hyperpolarisation event identification**

After observing transient hyperpolarisations during experiments, traces were searched, and hyperpolarisations were identified manually. 10 hyperpolarisations from 9 traces recorded from rat neuronal dendrites were identified. Width was defined as the width of the hyperpolarisation event at half-prominence, and the baseline was defined as an average of the signal for 100 ms before the event.

#### **Sustained hyperpolarisation periods**

Periods of sustained hyperpolarisation were identified manually during the process of searching for hyperpolarisation events. In total, 36 events were identified from 49 traces. The amplitude of long hyperpolarisation was defined as the difference between the baseline and the minimum voltage value in that segment. The baseline was defined as the average voltage for 1 s before a period of long hyperpolarisation.

#### **Principal component analysis**

132 The Principal axes presented in Fig. 2d were defined as the eigenvector of the inertia tensor  
 133  $\hat{\gamma}$ . The baseline axis of Fig. 2d is the  $x$ -axis and the peak amplitude is the  $y$ -axis. The inertia  
 134 tensor is given by diagonalizing the matrix:  
 135

$$136 \quad \hat{\gamma} = \begin{pmatrix} I_{xx} & -I_{xy} \\ -I_{yx} & I_{yy} \end{pmatrix},$$

$$137 \quad \text{where the entries are } I_{xx} = \sum_i (x_i - x_0)^2, \quad I_{yy} = \sum_i (y_i - y_0)^2, \quad I_{xy} = \sum_i (y_i - y_0)(x_i - x_0) \text{ and } x_i, y_i -$$

138 are positions of experimental points (baseline and amplitude peak respectively);  $x_0, y_0$  – are  
 139 the coordinates for the center of the mass of the experimental data points.  
 140

#### 141 **Binned event count**

142 To quantify activity levels in Fig. 6d, recordings were divided into 10 s bins and the number of  
 143 peaks detected per bin (following the single event detection protocol described above) was  
 144 counted, e.g., if 14 events were detected in a 10 s window then that binned event count is  
 145 14.  
 146

#### 147 **Distance from soma**

148 The distance between the nanopipette-dendrite point of contact and the cell soma used for  
 149 figure S2 was determined in Fiji by measuring from the nanopipette tip along the targeted  
 150 dendrite to the soma centre using the segmented line tool in pixel-size calibrated images.  
 151

152 **Table S1:** Parameters used to fabricate nanopipettes with the P2000. Parameters are  
 153 dimensionless unless stated otherwise.

HEAT	VEL	DEL	PUL
480	25	170	200

154

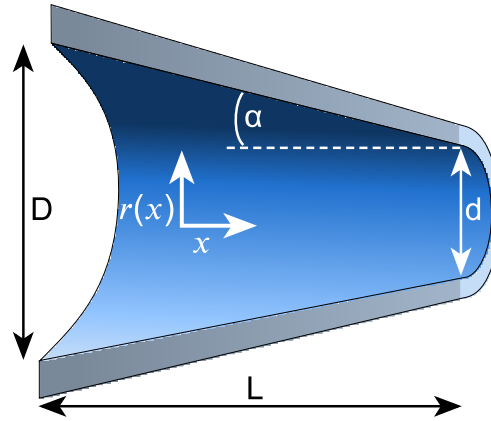


**Figure S1. Nanopipette tip geometry.** A conical frustum tapers over a length of  $L$  at a taper angle of  $\alpha$ . The diameter of the frustum base is  $D$  and the opening diameter is  $d$ . The radius,  $r$ , varies with position along the pipette axis,  $x$ .

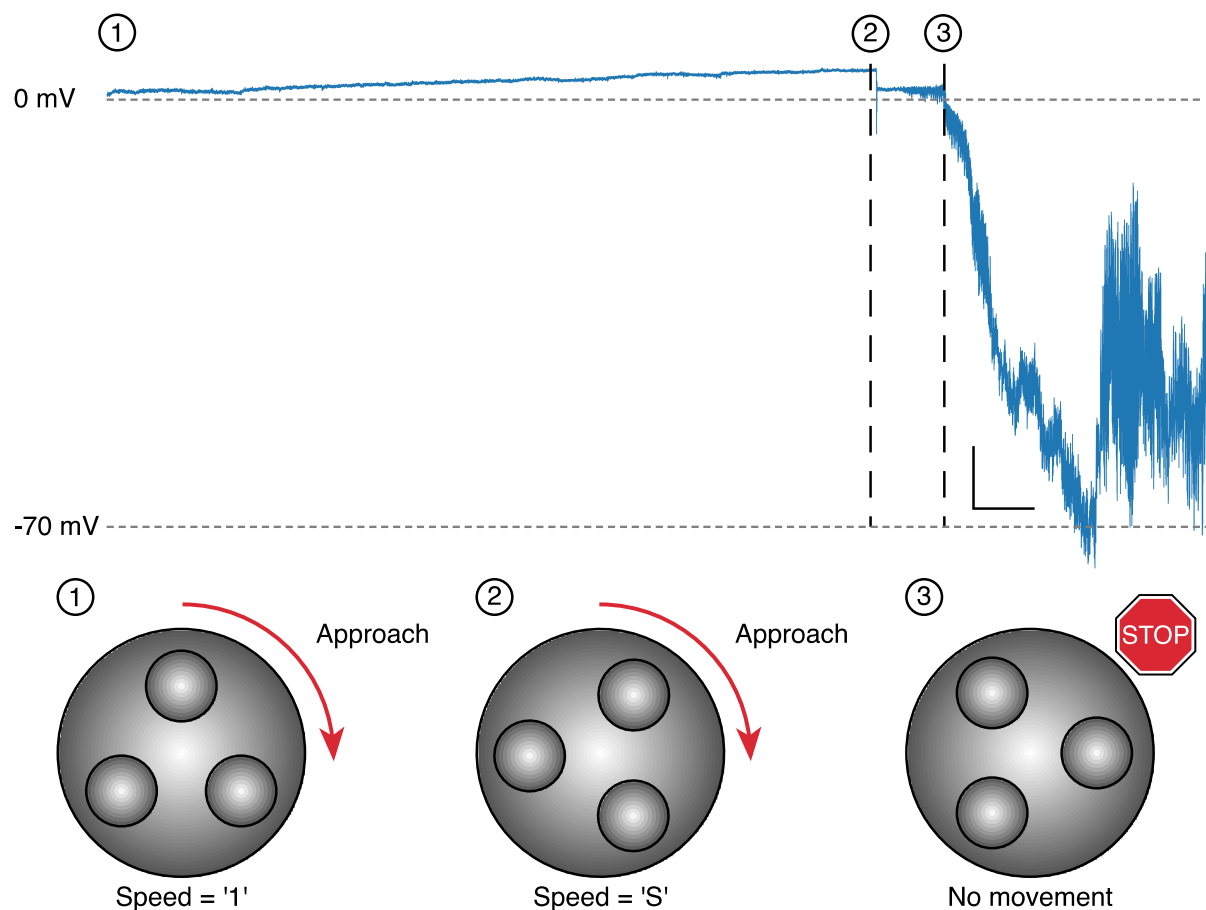
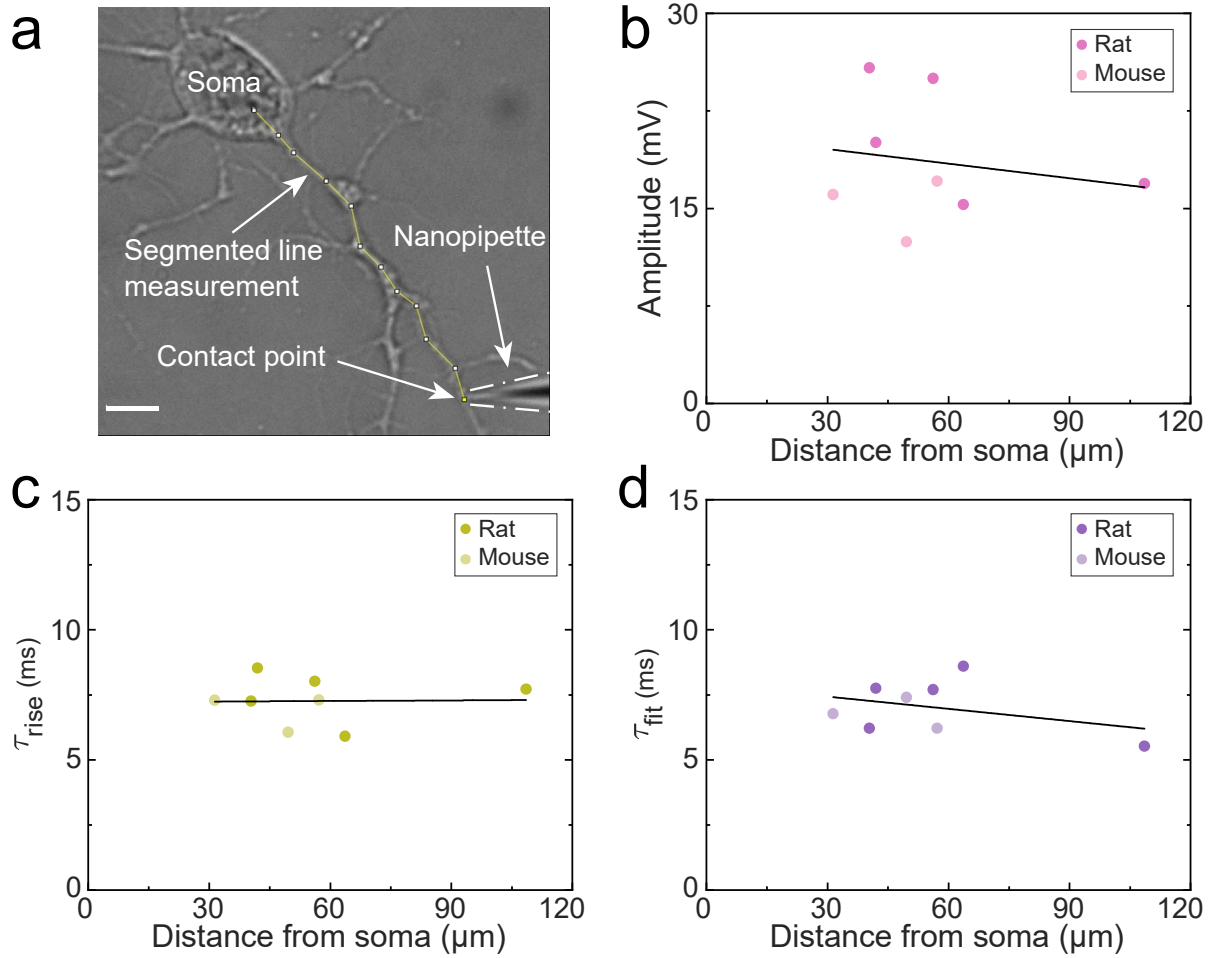


**Figure S2. Final approach to contact a dendrite.** Trace shows the recorded potential as the nanopipette is brought closer in the final approach to the cell before patching, with the approach divided into 3 steps. Step 1: At this point the cell is in focus and the nanopipette is clearly visible but out of focus above the cell. The potential is close to 0 mV and the manipulator is operated at speed of '1'. Step 2: Some contact is made, there is a step change in the potential, of about 5 mV in amplitude. The speed is reduced to 'S' and the approach continues, while carefully monitoring the potential for any changes. Step 3: The potential sharply decreases, approach is stopped immediately. Activity is now being recorded from the target dendrite. Scale bar 10 mV 2.5 s.



177  
 178 **Figure S3. Voltage dynamics with varying distance from soma.** (a) Schematic of distance from  
 179 soma measurement. Scale bar 5  $\mu\text{m}$ . (b) Mean event amplitudes determined from recordings  
 180 of rat and mouse neuronal dendrites plotted against the distance between the nanopipette-  
 181 dendrite contact point and the soma of the target neuron (distance from soma). (c) Mean rise  
 182 times of recorded events as they vary with distance from soma. (d) Mean decay times of  
 183 recorded events with distance from soma of the target neurons. Linear fit R-square, (b), 0.04,  
 184 (c) 0.02, (d) 0.13.  
 185

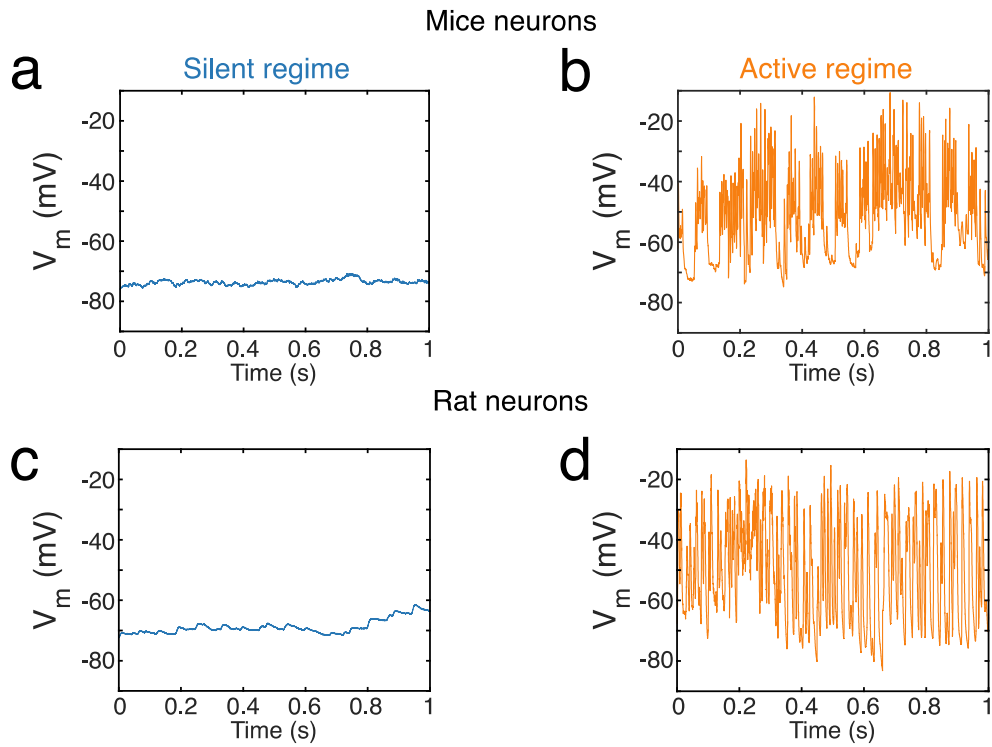


**Figure S4. Examples of silent and active regimes.** (a) Trace showing 1 s of the silent regime recorded from mouse neuronal dendrites. (b) Example of the high activity levels seen in the active regime recorded from mouse neuronal dendrites. (c) Quiet trace seen during the silent regime recorded from rat neuronal dendrites. (d) Example of the active regime observed in rat neuronal dendrites.